

# Shear-Mode Contact Splitting for a Microtextured Elastomer Film

By *Rebecca K. Kramer, Carmel Majidi, and Robert J. Wood\**

Texturing the surface of a PDMS film with microscale pillars has been shown to enhance shear adhesion to a rigid substrate by an order of magnitude when compared to untextured control films. In this study, it is shown that shear load is distributed uniformly among the contacts rather than concentrated on the contacts nearest the edge of the film-substrate interface, which is in contrast to the Kendall peel model for shearing substrates. The total shear strength of adhesion is thus estimated as the combined shear strength of each individual micro-contact. Shear-mode contact splitting is confirmed optically with experiments in which shear failure is observed through a glass coverslip.

Recent literature has suggested that texturing the surface of an elastic film may enhance adhesion to a rigid substrate. Theoretical studies have shown that introducing surface microstructures allows interfacial stress to be distributed to the edge of every feature, rather than concentrated at the blunt edge of the film-substrate interface.<sup>[1,2]</sup> For the case of a solitary surface contact, irregularities initiate crack propagation throughout the entire interface. In dividing the contact into finer sub-contacts, there is an increased tolerance of defects at individual contacts.<sup>[3–5]</sup> Contact splitting in a peel-test, for which one substrate is incision-patterned, has shown that a new crack must re-initiate at every incision.<sup>[6–8]</sup> Crack initiation from a film defect occurs at a load much higher than that required for propagation on a smooth unpatterned surface, yielding intermittent propagation for multiple defects and an overall increase in normal adhesion. Experimentally, this property has been manifested in fibrillar samples showing larger pull-off stress per unit contact area than non-fibrillar controls.<sup>[9–15]</sup> Furthermore, the role of fibrillar contact shape on adhesion of split contact surfaces has been shown to be notable.<sup>[14,15]</sup> An increased tip size, relative to the fibril base, seems to distribute stress singularities along the edge of the contact interface, delaying failure in adhesion.<sup>[13]</sup>

Textured surfaces have also been shown to greatly enhance friction.<sup>[16–22]</sup> High-friction, low-adhesion materials, which characterize the behavior of a 'directional' adhesive, are often inspired by gecko adhesion.<sup>[23]</sup> However, the mechanics of contact splitting between substrates in pure shear has thus far been elusive. The Kendall peel model predicts that the force required for slip between substrates in pure shear depends entirely on contact area width and is independent of length.<sup>[24]</sup>

[\*] R. K. Kramer, Dr. C. Majidi, and Prof. R. J. Wood  
School of Engineering and Applied Sciences  
Harvard University  
Cambridge, MA 02138 (USA)  
E-mail: rjwood@eecs.harvard.edu

DOI: 10.1002/adma.201000897

For a textured surface, we have found that redistributing stress to the edge of every contact results in an interfacial shear strength that scales with area rather than width.

In this work, we focus on low aspect-ratio (AR = 0.2) PDMS (polydimethylsiloxane, E ≈ 2 MPa) microstructures for drastically improved shear adhesion. The advantage of a low-aspect ratio is that it eliminates the bending moment on the adhesive bond and thus improves the interfacial fracture strength. The microstructure, which somewhat resembles the appearance of a solid hemisphere, is made in a one-step molding process that has been found to be highly repeatable. Shear adhesion is shown to increase by an order of magnitude when compared to an unpatterned PDMS surface. Four different geometries of square-packed microstructures were tested for shear adhesive strength, each varying either fibril diameter or center-to-center distance between fibrils (pitch): (1) 50 μm diameter, 100 μm pitch; (2) 100 μm diameter, 225 μm pitch; (3) 100 μm diameter, 250 μm pitch; (4) 100 μm diameter, 275 μm pitch. These four geometries were derived from limitations presented by fabrication and visualization methods, such that there was no mechanical coupling between neighboring contacts and the mode of interfacial failure could be observed with an optical microscope. Samples could be tested many times without damage to the fibrillar structures. The textured surface was found to allow interfacial stress to be distributed over a greater area, such that the critical shear load for detachment is controlled by fracture of the individual contacts. This mode of failure has been confirmed optically with experiments in which shear contact splitting is observed and shown to scale linearly with area.

Arrays of the PDMS fibrillar holes of the desired dimensions were patterned onto silicon wafers by means of standard photolithography processes.<sup>[15,25,26]</sup> A simple mask array of dots was used, the diameter of which determines the diameter of the final structures, and choice of photoresist and spin rate determine the subsequent depth of the features. Although other recipes may be used to obtain a similar result, the exact method implemented for the structures described in this paper is given here. Photoresist (SU-8 2010) was spun onto a clean wafer at 500 rpm for 5 seconds (spread), followed by 1000 rpm for 33 seconds (spin). The wafer was then placed on a hot plate at 65 °C for 1 minute and 95 °C for 3 minutes. The wafer was then underexposed in a UV flood exposure (lamp intensity ≈ 15 mW/cm<sup>2</sup>) for 4.1 seconds and post-baked for 4.5 minutes at 95 °C.

Underexposure is the key step in fabricating the desired overhanging structure. Because the photoresist layer was not fully exposed close to the wafer, subsequent developer (SU-8 developer) steps allowed the sidewalls of the fibril mold to wear away. The resulting mold has a bowl-like cross-section, as shown in Figure 1.

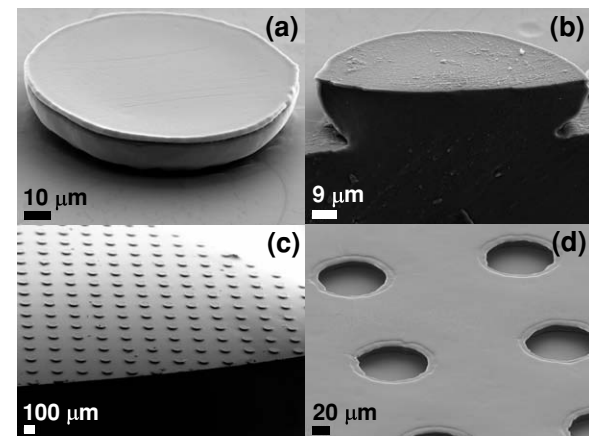


**Figure 1.** SEM images of PDMS microstructures. a) A single microstructure, about 100  $\mu\text{m}$  in diameter and 20  $\mu\text{m}$  in height. b) Cross-sectional view of a single microstructure, displaying its half-circular profile and slightly concave tip. c) Microstructure array displaying one out of four tested geometries. Microstructure diameter is 100  $\mu\text{m}$  and center-to-center distance between structures is 250  $\mu\text{m}$ . d) Silicon master from which PDMS structures were molded, fabricated from SU-8 on a silicon wafer.

After the silicon wafer was patterned, it was used to mold PDMS. A hydrophobic monolayer was introduced by vapor deposition to ensure easy removal of the subsequent mold. The patterned wafer was placed in an evacuated chamber (~20 mTorr) with an open vessel containing a few drops of Trichloro(1H,1H,2H,2H-perfluoroctyl)silane (Aldrich) for  $\geq 3$  hours. PDMS (Sylgard 184; Dow Corning, Midland, MI) was cast in liquid form (10:1 mass ratio of elastomer base to curing agent) against the silicon wafer. The PDMS was then cross-linked in the mold by oven-curing at ~65  $^{\circ}\text{C}$  overnight. The fibrillar PDMS sample was then removed manually from the master. The resulting fibrils were approximately 20  $\mu\text{m}$  in height and equal to the mask-dot-diameter at the tip.

Macroscale shear tests consisted of pure sliding with no normal compressive load. Shear adhesion between PDMS samples and glass slides (Microscope Slides, Fisher Scientific, 1 mm thick) was measured using an Instron Materials Testing System (model 5544A) in tensile extension mode. The glass slides were pre-cleaned with isopropanol and deionized water to remove dust before testing. Initial contact area was defined as the product of the nominal width and length of the interface, as opposed to the (considerably smaller) true area of contact. Samples were sufficiently preloaded to ensure adhesion over the nominal contact area, although it was often found that negligible force was required. Samples were sheared at a consistent strain rate of 60 mm/s until slip-failure. For completeness, several samples were tested at varying strain rates to verify that strain rate did not affect the outcome of the experiments.

For each of the four geometries, at least ten samples were tested in order to obtain an average measure of maximum shear load before detachment. For each sample, contact width and length were varied, and each test was repeated at least five

times to check for consistency. When necessary, PDMS samples were cleaned with Scotch tape to remove dust, which did not damage the microstructures.

Shear force increased as the microstructured sample was pulled in pure shear with no normal load. Maximum shear force before slip-failure was recorded and can be seen in **Figure 2**. For each textured sample tested, the opposite unpatterned side of the PDMS was consequently tested for a direct comparison. In all tests, the textured surface of the PDMS enhanced the interfacial shear strength by approximately an order of magnitude. In some cases, the PDMS sample would actually tear, or slip within the gripper in which it was secured, before it could fail in shear adhesion.

Shear strength dependency on the width and length of the contact zone was tested. According to Kendall's peel model, the interfacial shear strength,  $V_0$ , between an elastic film and rigid substrate will be linearly proportional to the width,  $w$ , of the contact zone and independent of the contact length,  $L$ , along the direction of applied shear.<sup>[24]</sup> While Kendall's peel model is roughly consistent with the measurements for the unpatterned sample, it is clearly violated for the micropatterned samples. As demonstrated in **Figure 3b**, the shear strength of the micropatterned interface depends equally on the length and width of the nominal contact zone. This suggests that shear adhesion is controlled by contact throughout the area of the interface rather than just along the peel front.

The adhesion of smooth PDMS to a glass substrate is limited by fracture, which propagates through the interface when the applied shear force,  $V$ , exceeds a critical value,  $V_0$ . However,

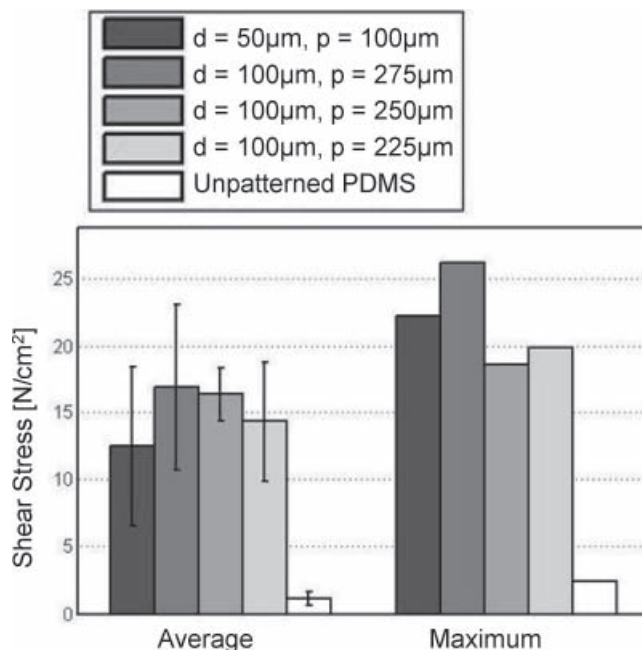


**Figure 2.** On the left: average shear strength of samples of different pattern geometries and unpatterned PDMS. The error bars span one standard deviation. On the right: the maximum shear strength observed, demonstrating the full capabilities of the microstructures.

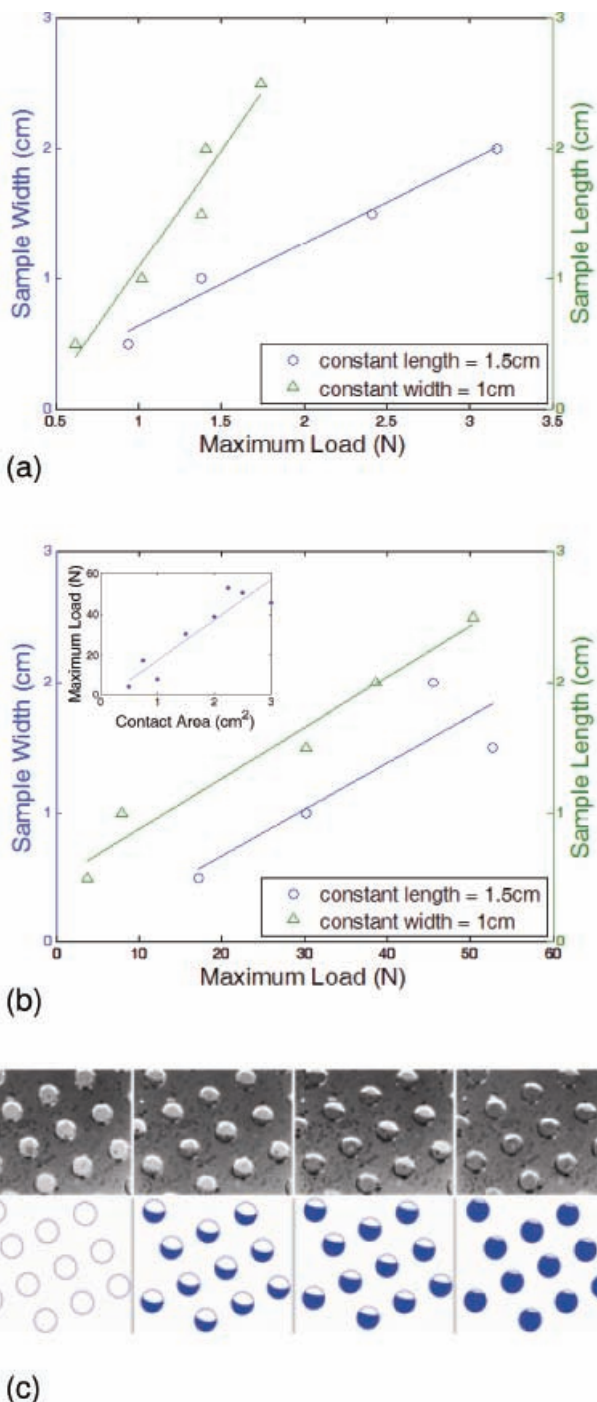


**Figure 3.** a,b) Maximum shear force dependence on sample width and length for (a) an unpatterned PDMS film and (b) a micropatterned PDMS film. Inset: Shear force scales linearly with area for patterned samples. c) Still frames (enhanced contrast) from top-down video of an array of the PDMS microstructures under pure shear. The microstructures are adhered to a glass slide, which is being steadily moved in the upward (slightly right) direction. At the critical shear load, a stress concentration at the edge opposite the direction of the shear force causes an interfacial crack to propagate across each microstructure in the array simultaneously. Crack propagation can be seen by the color contrast between adhered and detached surfaces. An illustrative sequence of images is provided for clarity.

texturing the surface of the PDMS with bowl-shaped microstructures allows the interfacial stress to be distributed over a greater area. In this case, the array of microstructures forms a relatively soft interface that allows shear load to be uniformly distributed among the microscale contacts. Thus, the critical shear load,  $V_0$ , for detachment is controlled by fracture of the individual micro-contacts. These contacts fracture simultaneously when the total applied shear force,  $V$ , reaches a critical value,  $V_0$ . This mode of failure is confirmed optically with experiments in which shear failure is observed through a glass coverslip. Referring to Figure 3c, failure occurs when a peel front moves through each interface in the direction opposite the external shear force.

As the experimental observations in Figure 3 suggest, the micropatterned samples should have a shear strength  $V_0 = \rho w L v_0$ , where  $\rho$  is the area density of the micropillars and  $v_0$  is the shear strength of each individual contact. For the 50  $\mu\text{m}$  diameter pillars,  $\rho = 10^4 \text{ cm}^{-2}$  and the nominal shear strength,  $V_0/wL$ , has an average value of 12 N/cm<sup>2</sup>. Therefore, the shear strength of each contact is approximately  $v_0 = 1.2 \text{ mN}$ . According to the classical adhesion theory of friction<sup>[27]</sup> and experiments with nano- and microscale indenters<sup>[28]</sup> the shear strength of a micro or nano-sized contact is expected to be proportional to the real area of contact. With the current experiments, however, the variation in real contact area among the different geometries is less than the variation in the shear strength measured among patterned samples with the same geometry. Therefore, these results do not independently confirm or contradict the scaling of adhesion with real contact area. Instead, they demonstrate that the shear strength of each patterned sample is controlled by distributed load sharing rather than conventional peeling and varies only moderately (~10%) with repeated testing.

We have not attempted to identify the reason why different samples of the same geometry (i.e. same pillar radius, pillar height, film width, film length, and film thickness) exhibit different absolute values of shear strength. We suspect that a combination of other factors associated with PDMS such as embedded electrostatic charge,<sup>[29]</sup> dwell time,<sup>[30]</sup> surface roughness,<sup>[31]</sup> and aging<sup>[32]</sup> may contribute to this variation. However, more rigorous scientific testing will be required to identify the predominate causes.

In summary, experimental measurements demonstrate that texturing the surface of the PDMS can enhance the shear strength of the interface by an order of magnitude. By uniformly distributing shear load among individual contacts, micropatterning eliminates the large stress concentration that exists along the width-wise peel front of an unpatterned interface. Instead, the stress concentration is divided into much smaller concentrations at the edge of each contact and so greater total force can be supported before bond failure occurs. As shown in Figure 3c, failure corresponds to the simultaneous detachment of each microstructured contact as individual peel fronts propagate in the direction opposite the applied force.

The shear strength of the micropatterned samples is found to scale with contact area and not width, as would be predicted by Kendall peel theory. This scaling behavior is consistent with other systems in which adhesion is improved through contact splitting.<sup>[1–8]</sup> Shear measurements and optical observations suggest that the interface has a shear strength  $V_0 = \rho w L v_0$ , where

$\rho = 1/p^2$  is the microstructure array density,  $p$  is the pitch length,  $w$  and  $L$  are the width and length of the nominal contact area, and  $v_0$  is the shear strength of each microcontact. Further analysis and numerical simulation will be required to identify microstructure geometries that would improve  $v_0$ .

## Acknowledgements

The authors gratefully acknowledge support from the National Science Foundation (award number DMR-0820484). Any opinions, findings and conclusions or recommendations expressed in this material are those of the authors and do not necessarily reflect those of the National Science Foundation. R. Kramer thanks the NSF Graduate Fellowship Program for financial support.

Received: March 13, 2010  
Published online: June 11, 2010

- [1] A. Peressadko, S. Gorb, *J. Adhes.* **2004**, *80*, 247.
- [2] C. Y. Hui, N. J. Glassmaker, T. Tang, A. Jagota, *J. R. Soc. Interface* **2004**, *1*, 12.
- [3] T. Tang, C. Y. Hui, N. J. Glassmaker, *J. R. Soc. Interface* **2005**, *2*, 505.
- [4] H. Gao, X. Wang, H. Yao, S. Gorb, E. Arzt, *Mechan. Mater.* **2005**, *37*, 275.
- [5] H. Gao, H. Yao, *Proc. Natl. Acad. Sci. USA* **2004**, *101*, 7851.
- [6] A. Ghatak, L. Mahadevan, M. K. Chaudhury, *Langmuir* **2005**, *21*, 1277.
- [7] A. Ghatak, L. Mahadevan, J. Y. Chung, M. K. Chaudhury, V. Shenoy, *Proc. R. Soc. A* **2004**, *460*, 2725.
- [8] J. Y. Chung, M. K. Chaudhury, *J. R. Soc. Interface* **2005**, *2*, 55.
- [9] A. K. Geim, S. V. Dubonos, IV Grigorieva, K. S. Novoselov, A. A. Zhukov, S. Y. Shapoval, *Nat. Mater.* **2003**, *2*, 461.
- [10] S. Kim, M. Sitti, *Appl. Phys. Lett.* **2006**, *89*, 261911.
- [11] N. J. Glassmaker, A. Jagota, C. Y. Hui, J. Kim, *J. R. Soc. Interface* **2004**, *1*, 23.
- [12] N. J. Glassmaker, A. Jagota, C. Y. Hui, W. L. Noderer, M. K. Chaudhury, *Proc. Nati. Acad. Sci. USA* **2007**, *104*, 10786.
- [13] A. V. Spuskanyuk, R. M. McMeeking, V. S. Deshpande, E. Arzt, *Acta Biomater.* **2008**, *4*, 1669.
- [14] S. Gorb, M. Varenberg, A. Peressadko, J. Tuma, *J. R. Soc. Interface* **2007**, *4*, 271.
- [15] A. del Campo, C. Greiner, E. Arzt, *Langmuir* **2007**, *23*, 10235.
- [16] S. Kim, B. Aksak, M. Sitti, *Appl. Phys. Lett.* **2007**, *91*, 221913.
- [17] C. Majidi, R. E. Gro\_, Y. Maeno, B. Schubert, S. Baek, B. Bush, R. Maboudian, N. Gravish, M. Wilkinson, K. Autumn, *Phys. Rev. Lett.* **2006**, *97*, 76103.
- [18] L. Ge, S. Sethi, L. Ci, P. M. Ajayan, A. Dhinojwala, *Proc. Natl. Acad. Sci. USA* **2007**, *104*, 10792.
- [19] P. L. Dickrell, S. B. Sinnott, D. W. Hahn, N. R. Raravikar, L. S. Schadler, P. M. Ajayan, W. G. Sawyer, *Tribol. Lett.* **2005**, *18*, 59.
- [20] J. Lee, C. Majidi, B. Schubert, R. S. Fearing, *J. R. Soc. Interface* **2008**, *5*, 835.
- [21] M. P. Murphy, B. Aksak, M. Sitti, *Small* **2009**, *5*, 170.
- [22] M. Varenberg, S. Gorb, *J. R. Soc. Interface* **2007**, *4*, 721.
- [23] K. Autumn, *MRS Bull.* **2007**, *32*, 473.
- [24] K. Kendall, *J. Phys. D: Appl. Phys.* **1975**, *8*, 1449.
- [25] J. Davies, S. Haq, T. Hawke, J. P. Sargent, *Intl. J. Adhes. Adhes.* **2009**, *29*, 380.
- [26] H. E. Jeong, J. K. Lee, H. N. Kim, S. H. Moon, K. Y. Suh, *Proc. Natl. Acad. Sci. USA* **2009**, *106*, 5639.
- [27] E. Rabinowicz, *Friction and Wear of Materials*, Wiley-VCH, Weinheim **1965**.
- [28] K. L. Johnson, *Proc. R. Soc. A* **1997**, *453*, 163.
- [29] A. D. Roberts, *J. Phys. D: Appl. Phys.* **1977**, *10*, 1801.
- [30] A. D. Roberts, A. B. Othman, *Wear* **1977**, *42*, 119.
- [31] B. N. J. Persson, E. Tosatti, *J. Chem. Phys.* **2001**, *115*, 5597.
- [32] A. Kurian, S. Prasad, A. Dhinojwala, *Macromolecules* **2010**, *43*, 2438.